Estrous cycle modulates inhibition of dorsal motor nucleus

Boychuk, C.R., Halmos, K.Cs., Smith, B.N.
University of Kentucky, Collage of Medicine, Department of Physiology, Lexington, KY

INTRODUCTION

Although detailed mechanism(s) responsible are still controversial, two brain regions, the hypothalamus and the dorsal vagal complex (DVC), play critical roles in central energy homeostatic modulation. Injection of nutrient signals (e.g. insulin or glucose) into these regions can alter overall blood glucose through vagal activity. The DVC is made up of the dorsal motor nucleus of the vagus (DMV), the nucleus tractus solitarius (NTS) and area postrema. The DMV contains the cell bodies of neurons responsible for parasympathetic motor output to subdiaphragmatic viscera making them a final, central modulation point in parasympathetic activity. Inhibitory, GABAergic neurotransmission contributes significantly to vagal motor neuron activity. Elevating glucose in the DVC elevates blood glucose and influences descending parasympathetic motor drive through activation of inhibitory, GABAergic currents in males. A small body of evidence suggests that $GABA_A$ receptor activity exhibits sexually dimorphic regulation. This regulation is estrous cycle-dependent and occurs even in brain regions with no direct role in reproduction. However, no work to date has examined sex differences in or estrous cycle regulation of DMV neurons. Since other energy homeostatic signaling mechanisms demonstrate sexual dimorphism, these relationships need to be elucidated. Therefore, the present study investigated if estrous cycle modulates GABAergic neurotransmission to DMV neurons.

METHODS

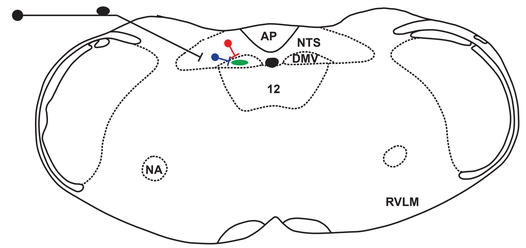

Figure 1: Illustration of the location of the DMV. Green oval represents the DMV neuron. Red and blue represent the GABAergic and glutamatergic innervations to the DMV from the nucleus tractus solitarius (NTS) respectively. Black represents the primary afferent. 12: hypoglossal nucleus; AP: area postrema; NA: nucleus ambiguus; RVLM: rostral ventral lateral medulla

IN VITRO ELECTROPHYSIOLOGY:

Experiments used 5-8 week old male and cycling female FVB mice, bred in-house. Estrus and diestrus was determined by vaginal smear. Anoestrous females were excluded.

On the day of experimentation, mice were decapitated after an overdose with isoflurane. Brain tissue was collected and placed in ice-cold artificial cerebral spinal fluid (aCSF) bubbled with 95% O_2-5% CO_2. The composition of aCSF was as follows (in mM): 124 NaCl, 3 KCL, 26 $NaHCO_3$, 11 glucose, 1.3 $CaCl_2$, and 1.3 $MgCl_2$. Slices of 300 µm were made to include the DMV. Slices were transferred to a holding chamber and incubated in oxygenated aCSF at 32-34ºC.

Whole-cell patch-clamp recordings were performed using glass pipettes (2-5MΩ) filled with a solution containing the following (in mM): 130 Cs+ -gluconate, 1 NaCL, 5 EGTA, 10 HEPES, 1 $MgCl_2$, 1 $CaCl_2$, 3 CsOH and 2-3-ATP (2mM) at a pH or 7.3. Identified DMV cells were voltage-clamped at a holding potential of 0 mV. Kynurenic acid (KYN; 1mM) was added to perfusate to isolate GABAergic currents.

All recordings were low-pass filtered at 3kHz and acquired digitally at 20 kHz. Mini-analysis software was used to measure inhibitory postsynaptic current (IPSC) frequency, amplitude, and area.

PCR:

In another subset of FVBs, 3-4 slices were generated and 1 mm punch (Miltex Inc., York, PA) was used to collect the dorsal vagal complex. Punches from one animal were pooled into one sample. All quantitative RT-PCR reactions were run in triplicate in 96-well optical grade plates using a 7500 Fast Real-Time PCR System (Applied Biosystems, Foster City, CA). Total volume for each run was 25µL containing 25ng of cDNA. The reaction times and temperature were 50°C for 2 mins, 95°C for 10 mins, followed by 50 cycles of 95°C for 15 s, and 60°C for 1 min. Primer and Taqman probe sets were purchased from Applied Biosystems. The sequences for each were generated from the listed references in GenBank: δ: Mm01266203 and β-actin: Mm00607939.

Supported By: R01 DK056132 to BNS

Mean sIPSC parameters are not modulated by estrous cycle

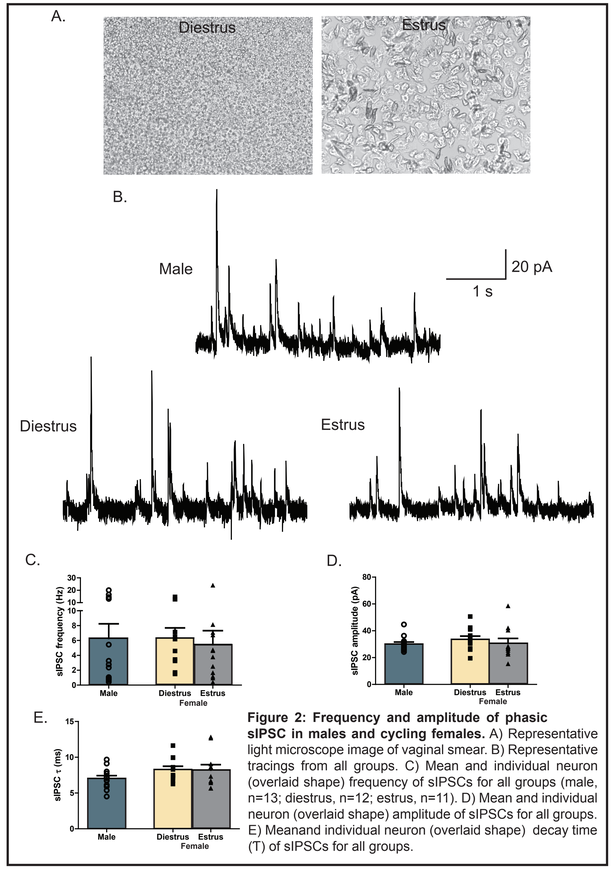

Figure 2: Frequency and amplitude of phasic sIPSC in males and cycling females. A) Representative light microscope image of vaginal smear. B) Representative tracings from all groups. C) Mean and individual neuron (overlaid shape) frequency of sIPSCs for all groups (male, n=13; diestrus, n=12; estrus, n=11). D) Mean and individual neuron (overlaid shape) amplitude of sIPSCs for all groups. E) Meanand individual neuron (overlaid shape) decay time (T) of sIPSCs for all groups.

Decreased phasic sIPSC variability during diestrus

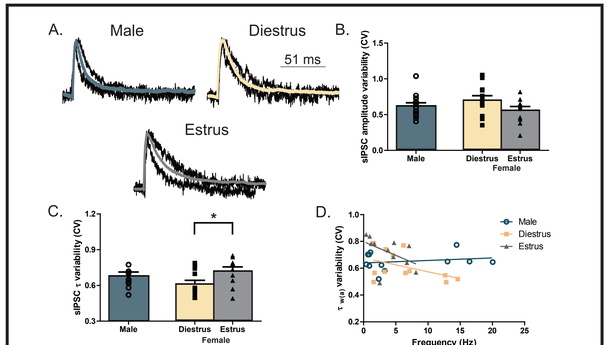

Figure 3: Variability of phasic sIPSCs' amplitude and decay time in males and cycling females. A) Representative tracings (scaled to amplitude) from one neuron per groups demonstrating decay time variability. B) Mean and individual neuron (overlaid shape) amplitude variability for all groups. (male, n=13; diestrus, n=12; estrus, n=11) C) Mean and individual neuron (overlaid shape) decay time variability for all groups. D) Correlation between decay time variability and frequency of sIPSCs. * significant difference (ANOVA with Tukey's)

Increased inhibitory tonic currents during diestrus

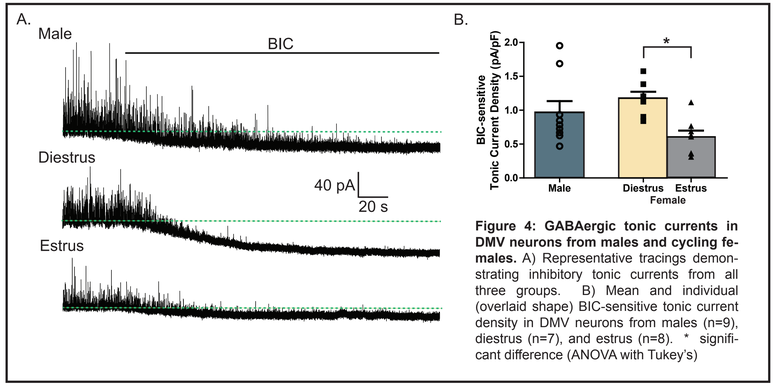

Figure 4: GABAergic tonic currents in DMV neurons from males and cycling females. A) Representative tracings demonstrating inhibitory tonic currents from all three groups. B) Mean and individual (overlaid shape) BIC-sensitive tonic current density in DMV neurons from males (n=9), diestrus (n=7), and estrus (n=8). * significant difference (ANOVA with Tukey's)

Decreased "THIP-Inducible" tonic currents during diestrus

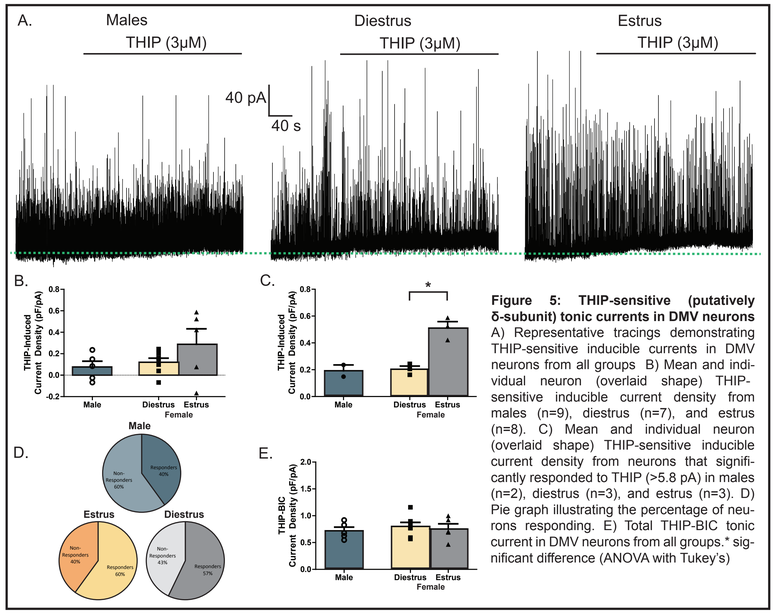

Figure 5: THIP-sensitive (putatively δ-subunit) tonic currents in DMV neurons A) Representative tracings demonstrating THIP-sensitive inducible currents in DMV neurons from all groups B) Mean and individual neuron (overlaid shape) THIP-sensitive inducible current density from males (n=9), diestrus (n=7), and estrus (n=8). C) Mean and individual neuron (overlaid shape) THIP-sensitive inducible current density from neurons that significantly responded to THIP (>5.8 pA) in males (n=2), diestrus (n=3), and estrus (n=3). D) Pie graph illustrating the percentage of neurons responding. E) Total THIP-BIC tonic current in DMV neurons from all groups.* significant difference (ANOVA with Tukey's)

Phasic sIPSC THIP-sensitivity is increased during diestrus

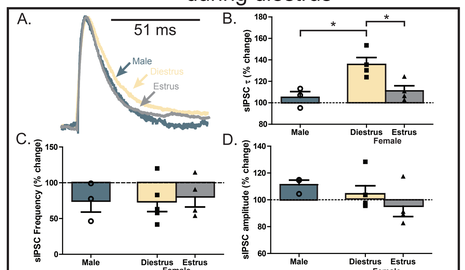

Figure 6: THIP-sensitivity of phasic currents. A) Representative IPSC from all groups (scaled to amplitude) during THIP bath application. B) Percent change in sIPSC decay time after THIP application. C) Percent change in sIPSC frequency after THIP application. C) Percent change in sIPSC amplitude after THIP application. * significant difference (ANOVA with Tukey's)

Sexually dimorphic $GABA_A$ receptor δ-subunit expression

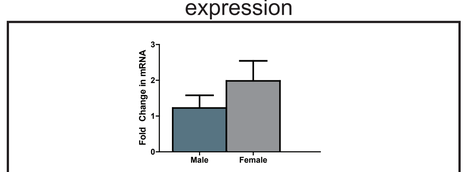

Figure 7: Preliminary data suggests that estrous females have increased mRNA expression profile of the $GABA_A$ receptor δ-subunit. Mean fold changes in the expression of δ-subunit in males (n=5) and estrous females (n=3).

Diabetes may differentially alter $GABA_A$ receptor δ-subunits in females

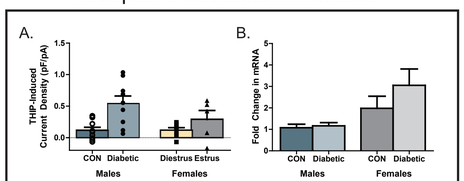

Figure 8: Females may be uniquely susceptible to diabetic GABAergic plasticity in the DMV. A) THIP-sensitive inducible tonic current in males (control, CON, vs. diabetic) compared to normal, cycling females. B) Mean fold changes in the expression of δ-subunit in CON males (n=8) and diabetic males (n=8) compared with estrous CON females (n=3) and diabetic estrous females (n=3)

CONCLUSIONS

1. Estrous cycle does not significantly modulate phasic sIPSC parameters. DMV neurons from females in diestrus have significantly less decay time variability than neurons from females in estrus. This is not likely mediated from an increased frequency of sIPSCs since frequency is not changed (figure 2) and frequency does not predict decay time variability. This is likely mediated through a reduced heterogeneity in postsynaptic receptor composition.

2. During diestrus, "resting" tonic $GABA_A$ receptor inhibitory currents in DMV neurons are significantly elevated. This elevated tonic current could be a result of either 1) elevated numbers of receptors peri-/extrasynaptic and/or 2) changes in receptor phosphorylation.

3. THIP-sensitive tonic currents in the DMV of estrous females are significantly elevated and demonstrate a significant "inducible" component. This elevated THIP-sensitivity increased the overall tonic current (THIP-BIC; figure 5) in estrous females, thereby "normalizing" them to the tonic currents demonstrated in DMV neurons from females in diestrus. It has been suggested that this "THIP-induced" current represents an unoccupied receptor population. Therefore, DMV neurons from estrus females may have a larger number of receptors that are not actively contributing to "resting" tonic currents, but are present in the membrane.

4. Preliminary data also suggests that the $GABA_A$ receptor δ-subunit expression in DMV neurons from estrous females is elevated compared to male counterparts. These increase in mRNA expression could be the driving force for the electrophysiological changes demonstrated here.

5. Overall, estrous cycle modulates inhibition in DMV neurons. Through a currently unknown mechanism(s), estrous cycle alters both phasic and tonic $GABA_A$ receptor activity. It was previously identified that experimentally-induced diabetes increases THIP-sensitivity in DMV neurons. Since estrous cycle also modulates similar neuronal physiology, females may have a unique susceptibility to diabetic perturbations of $GABA_A$ receptor activity in the DMV. This altered susceptibility could result in (or from) a sex difference in $GABA_A$ receptor expression.